minerals

MDPI

Article

Marine Phosphorites as Potential Resources for Heavy Rare Earth Elements and Yttrium

James R. Hein [1,*], Andrea Koschinsky [2], Mariah Mikesell [1], Kira Mizell [1,3], Craig R. Glenn [4] and Ray Wood [5]

1 Pacific Coastal and Marine Science Center, U.S. Geological Survey, 2885 Mission St., Santa Cruz, CA 95060, USA; mmikesell@usgs.gov (M.M.); kmizell@usgs.gov (K.M.)
2 Department of Physics and Earth Sciences, Jacobs University, Bremen, P.O. Box 750561, Bremen D-28725, Germany; a.koschinsky@jacobs-university.de
3 Ocean Sciences, University of California at Santa Cruz, Santa Cruz, CA 95064, USA
4 Department of Geology and Geophysics, School of Ocean and Earth Science and Technology, University of Hawaii, 1680 East West Rd., POST 701, Honolulu, HI 96822, USA; glenn@soest.hawaii.edu
5 Chief Operations Officer, Chatham Rock Phosphate, 93 The Terrace, Wellington 6011, New Zealand; raywood@crpl.co.nz
* Correspondence: jhein@usgs.gov; Tel.: +1-831-460-7419

Academic Editor: Adrian Jones
Received: 13 June 2016; Accepted: 17 August 2016; Published: 29 August 2016

Abstract: Marine phosphorites are known to concentrate rare earth elements and yttrium (REY) during early diagenetic formation. Much of the REY data available are decades old and incomplete, and there has not been a systematic study of REY distributions in marine phosphorite deposits that formed over a range of oceanic environments. Consequently, we initiated this study to determine if marine phosphorite deposits found in the global ocean host REY concentrations of high enough grade to be of economic interest. This paper addresses continental-margin (CM) and open-ocean seamount phosphorites. All 75 samples analyzed are composed predominantly of carbonate fluorapatite and minor detrital and authigenic minerals. CM phosphorites have low total REY contents (mean 161 ppm) and high heavy REY (HREY) complements (mean 49%), while seamount phosphorites have 4–6 times higher individual REY contents (except for Ce, which is subequal; mean ΣREY 727 ppm), and very high HREY complements (mean 60%). The predominant causes of higher concentrations and larger HREY complements in seamount phosphorites compared to CM phosphorites are age, changes in seawater REY concentrations over time, water depth of formation, changes in pH and complexing ligands, and differences in organic carbon content in the depositional environments. Potential ore deposits with high HREY complements, like the marine phosphorites analyzed here, could help supply the HREY needed for high-tech and green-tech applications without creating an oversupply of the LREY.

Keywords: marine phosphorite deposits; seamount phosphorite; continental-margin phosphorite; rare earth elements; heavy rare earth elements; yttrium; resources

1. Introduction

Rare earth elements (REE) plus yttrium (REY) are known to concentrate in marine phosphorite deposits during their formation, primarily through early diagenetic processes where carbonates are replaced by carbonate fluorapatite (CFA), which also precipitates in void space (e.g., [1,2]). However, much of the REY data available in the literature are decades old and incomplete, and there has not been a systematic study of REY distributions in marine phosphorite deposits that formed over a range of oceanic environments (e.g., [1–3]). Consequently, this study was initiated to determine

the range of REY concentrations hosted by marine phosphorite deposits from the modern global ocean and whether the deposits are of high enough grades to be of economic interest.

Phosphorites in the global ocean occur in three general environments, continental margins (CM: shelf, slope, banks, and plateaus), seamounts, especially the old (Cretaceous) seamounts in the NW Pacific, and lagoon/insular deposits (e.g., [4,5]). Research presented here addresses only the CM and seamount phosphorites. Our global dataset includes typical shallow-water continental-margin, upwelling-zone phosphorites, and deep-water seamount phosphorites collected from the Pacific and Atlantic Oceans (Table S1, Figure 1).

Similar studies have been completed for land-based phosphorite deposits, with positive results as to the resource potential of REY as a byproduct or co-product of the focus phosphate mining (e.g., [6,7]). However, recovery of these land-based REY would require the addition of costly infrastructure and changes in extractive processing to the existing phosphate mining operations. For example, it would be beneficial to change the dissolution acid from sulfuric acid, which produces phosphogypsum as a waste product, to hydrochloric acid. This would alleviate processing a second solid for recovery of the REY partitioned into the phosphogypsum phase (e.g., [6,8]). Production of REY as a byproduct or co-product of phosphate mining needs to be considered in the early stages of planning for a new terrestrial or marine mining operation. With this in mind, three CM areas have been leased in the global ocean for exploration for marine phosphorites: Chatham Rise off New Zealand by Chatham Rock Phosphate Ltd. (Wellington, New Zealand); offshore Baja California, Mexico by Odyssey Marine Exploration and Exploraciones Oceanicas; and on the shelf off Namibia by Namibian Marine Phosphate Ltd. Again, consideration of REY as a byproduct at an early planning stage for a marine phosphorite operation would be warranted should extraction of the REY be determined to be economic.

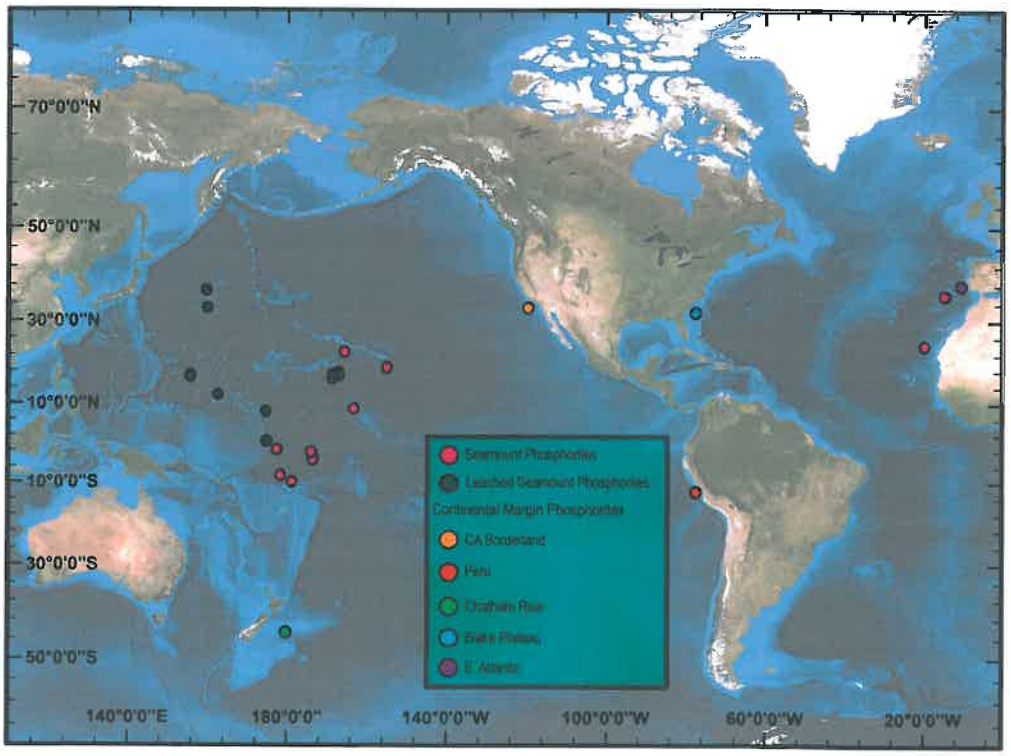

Figure 1. Location of samples used in this study. See Table S1 for coordinates.

The large land-based carbonatite REY ores contain more than 99% light REY (LREY) and new mines put into operation for recovery of the undersupplied heavy (HREY) as a consequence could create an oversupply of LREY to the market (e.g., [6]). Consequently, a search for deposits with the

largest HREY/LREY ratios would help alleviate the supply problem and marine phosphorites might be able to fill that need. Here, we define the LREE as La through Sm and the HREY as Eu through Lu including Y. We use this division because there is a clear break in the abundance of the REY between Sm and Eu in typical large land-based REY deposits that supply most of the REY used worldwide. The average LREE complement from the carbonatite ores supply a resource about three orders of magnitude larger than the HREY complement (e.g., [9]).

2. Samples and Methods

2.1. Sample Collection

Phosphorites were collected from dredge hauls taken during various cruises, except Johnson Sealink (JSL) samples were collected by manned submersible. Phosphorite samples were selected based on geographic location and major element concentrations. Our global dataset includes typical shallow-water (<1000 m) CM, upwelling-zone phosphorites from the east Pacific (southern California Borderland, n = 10; Peru margin, n = 10), Chatham Rise in the southwest Pacific (n = 15), Blake Plateau in the NW Atlantic (n = 10), and a NE Atlantic bank (n = 1 leached sample), and typical deep-water (1400 to ~3000 m) seamount phosphorites collected throughout the global ocean (n = 12 untreated and n = 18 leached samples to remove calcite; Table S1, Figures 1 and 2).

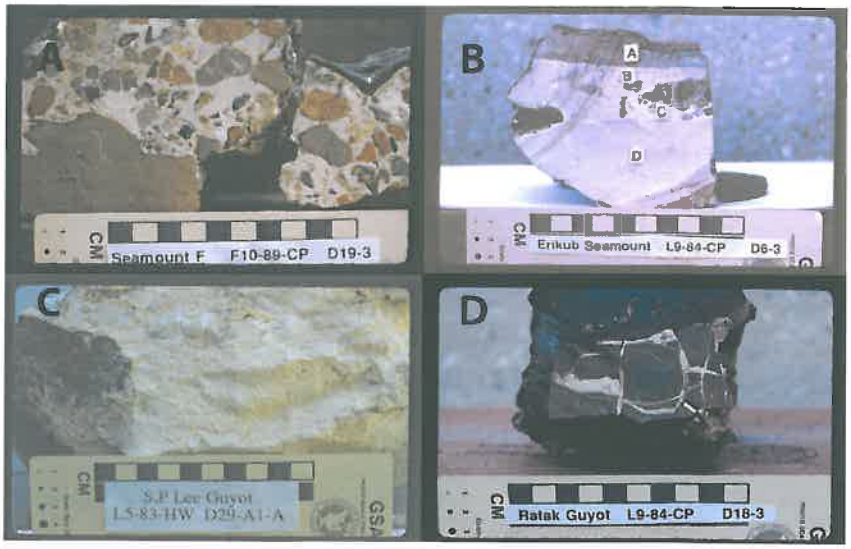

Figure 2. Photographs of seamount phosphorites: **(A)** cement-supported breccia; cement from carbonate fluorapatite (CFA)-replaced pelagic foraminifera matrix. **(B)** Massive, layered **(A–D)**, recrystallized phosphorite; protolith cannot be distinguished, low porosity. **(C)** Massive bed of CFA-replaced foraminifera, with nearly pristine microfossil structure; minor rim cement on foraminifera indurates the rock; very high porosity. **(D)** CFA-replaced carbonate sand that filled fractures in basalt. Note Fe-Mn crust on at least one surface of each sample.

Several seamount samples (Table S1) from water depths >3000 m may have been displaced downslope and collected as talus. In situ phosphatization on seamounts usually occurred at water depths of less than 2500 m, rarely to 3000 m [4,10].

The southern California borderland CM phosphorite samples are composed of breccia and sandstone cemented and replaced by CFA (Figure S1A). These Borderland deposits include phosphorite slabs and phosphorite fragments that vary from pale-brown to dark brown and black, and the surface is generally polished and smooth. The Peru CM phosphorite samples are cobble conglomeritic hardground crusts that form slabs and fragments derived from cementation and replacement

of carbonates by CFA, and that vary from black to pale brown, dark brown, and green-brown. A rough surface texture was inherited from the host clastic rock, and a few samples are polished. Several samples contain many small vugs, some filled with glauconite. These and similar samples from the region are described by [11,12]. The Chatham Rise phosphorite samples are polished pebbles of carbonates that were cemented and replaced by CFA (Figure S1B). The deposit was initially composed of phosphorite slabs that were subsequently fragmented by iceberg gouging during sea-level low-stands [13]. The phosphorite pebbles are typically dark brown and interspersed with off-white shell fragments. Blake Plateau CM phosphorite samples are composed of carbonates and breccia cemented and replaced by CFA, with predominantly well-polished phosphorite fragments and some phosphorite slabs. Samples are pale brown, pinkish-brown, and dark brown, and surfaces vary from polished and smooth to flaky. The seamount phosphorite samples are predominantly pelagic and reef carbonates cemented and replaced by CFA. These deposits are massive to layered fine-grained replaced foraminiferal sands, or replaced breccias (replaced reef material), and vary from pale brown, dark brown, pinkish pale brown, to gray, and typically have a Fe-Mn crust on the upper surface (Figure 2). Some samples are porous and others are very dense.

2.2. *Sample Preparation and Analyses*

One CM and 18 seamount samples were leached using 0.5 M triammonium citrate and 30% H_2O_2 to remove calcite and organic matter [4], leaving pure CFA in most of those samples based on X-ray diffraction (XRD) analysis (Tables 1 and 2); trace minerals below detection limit could be present. Those samples were leached so that the pure CFA could be dated using Sr isotopes [4]. In addition, some samples from all the locations were partially impregnated or coated with impurities such as Fe and Mn oxides, which were mechanically removed prior to mineralogical and chemical analyses. The phosphorite samples were then ground to <75 µm prior to XRD and chemical analyses, using both a shatter box, where the sample was contained in a ceramic dish, and an IKA A11 analytical mill.

Table 1. XRD mineralogy of phosphorites from seamounts [1].

Cruise ID	Sample ID	Major [2]	Moderate	Minor
AVON02	11-Massive	CFA	calcite	--
AVON02	11-Porous	CFA	--	calcite
AVON02	55-13	CFA	--	K-feldspar, chlorite
F10-89-CP	D10-17	CFA	--	--
F7-86-HW	CD19-1A	CFA	--	calcite, quartz, plagioclase
F7-86-HW	CD30-8	CFA	plagioclase	chlorite
TN037	D10-M-1	CFA	--	phillipsite, quartz
TN037	D12-2	CFA	--	quartz
TUNES6	D32-6	CFA	plagioclase	chlorite, smectite, sepiolite
TUNES6	D32-9	CFA	calcite	barite
V2-91-CP	D4-12	CFA	--	K-feldspar, smectite, amphibole
V2-91-CP	D7-8	CFA	--	quartz, ilmenite, palygorskite
Leached Samples [3]				
SO66	26 DSR 1	CFA	--	--
SO66	26 DSR 2	CFA	--	--
SO66 [4]	28 DSR 6	CFA	--	--
SO66	29 DSR 5	CFA	--	phillipsite
SO66	50 DSR 3	CFA	--	--
SO66	61 DSR 1	CFA	--	--
SO66 [4]	69 DSO 2	CFA	phillipsite	--
SO66	80 DSK 6	CFA	--	--
SO66	85 DSK 1	CFA	--	--
L5-83-HW [4]	D5-A3-2	CFA	--	--
L5-83-HW [4]	D29-A1-b	CFA	--	--
F7-86-HW [4]	CD14-2D	CFA	--	--
F2-88-HW [4]	D12-1A	CFA	--	quartz
F2-88-HW [4]	D12-5	CFA	--	quartz
SO83	64 GTV 1	CFA	--	--
SO83	118 GTV 6	CFA	--	--
SO83	126 GTV 3	CFA	--	--

[1] Major >25%; Moderate 5%–25%; Minor <5%; [2] CFA = carbonate fluorapatite; [3] Samples treated with 0.5 M triammonium citrate and 30% H_2O_2; [4] Mineralogy of sample did not change after leaching treatment; -- means not present.

Table 2. XRD Mineralogy of phosphorites from continental margins [1].

Cruise ID	Sample ID	Major [2]	Moderate	Minor
CA Borderland				
L-1-74-SC	LCB-14-A	CFA	Px	analcime, quartz
L-1-74-SC	LCB-14-B	CFA	Px, plagioclase	analcime
L-1-74-SC	LCB-1-4B	CFA	–	quartz, dolomite
L-1-74-SC	LCB-1-4C	CFA	quartz, plagioclase	–
L-1-74-SC	LCB-20-6C	CFA	plagioclase	quartz
L-1-74-SC	LCB-20-8B	CFA	–	Quartz (?)
L-2-76-SC	CD281-A	CFA	–	quartz
L-2-76-SC	CD281-B	CFA	–	Plagioclase (?)
L-2-76-SC	CD350-A	CFA	–	glauconite or illite, quartz (?)
L-2-76-SC	CD350-B	CFA	–	quartz, glauconite or illite
Peru Margin				
JSL	3350-1a	CFA	quartz, plagioclase	–
JSL	3350-1b	CFA	quartz, plagioclase	Illite (?), amphibole (?)
JSL	3352-4	CFA	plagioclase, quartz	–
JSL	3355-2	CFA	quartz, plagioclase	–
JSL	3363-4	CFA	quartz, plagioclase	–
JSL	3365-2	CFA	quartz	–
JSL	3372-1	CFA, quartz	plagioclase, pyrite	–
JSL	3365	CFA	plagioclase, quartz	–
JSL	3352-6	CFA	plagioclase	quartz
RC-2306	1-2, GS-1	CFA	plagioclase, Px, quartz	K-feldspar, glauconite
Chatham Rise				
NA	DD9+2-8	CFA	ASi	glauconite, pyrite (?)
NA	DD9+8	CFA, calcite	–	plagioclase, glauconite, quartz
NA	DD16+2-8	CFA	calcite	quartz, glauconite, pyrite
NA	DD16+8	CFA	calcite, goethite	quartz, glauconite
NA	DD19+2-8	CFA	calcite, ASi	glauconite, pyrite
NA	DD19+8	CFA	calcite, plagioclase	quartz, glauconite
NA	DD21+2-8	CFA	ASi	calcite, glauconite, pyrite (?)
Chatham Rise				
NA	DD21+8	CFA	calcite	goethite, pyrite, plagioclase, glauconite (?)
NA	DD22+2-8	CFA	calcite	quartz, glauconite, pyrite (?)
NA	DD22+8	CFA, calcite	plagioclase	–
NA	DD23+2-8	CFA	calcite, ASi	pyrite, glauconite, quartz (?)
NA	DD23+8	CFA, calcite	–	glauconite or illite
NA	DD24+2-8	aragonite, calcite	CFA	plagioclase, glauconite, chlorite (?)
NA	DD24+8	CFA, calcite	–	illite/smectite (mixed layer) (?)
Blake Plateau				
GOS 74	2397-A	CFA	quartz, calcite	glauconite
GOS 74	2397-B	CFA	calcite	quartz, glauconite or illite
GOS 74	2399-A	CFA	calcite, goethite	glauconite or illite
GOS 74	2399-B	CFA	calcite	glauconite or illite
GOS 74	2476-A	CFA, calcite	–	quartz
GOS 74	2476-B	CFA, calcite	–	k-feldspar, birnessite
GOS 74	2480	CFA	calcite	glauconite or illite, quartz, birnessite
GOS 74	2485	CFA	calcite	glauconite or illite, quartz
CHN46-1	Station 15-2	CFA	calcite, 10 Å manganate	–
AT266	D42-4	CFA	calcite, 10 Å manganate	analcime
E. Atlantic [3]				
SO83	23 GTV II A3	CFA	–	quartz

[1] Major >25%; Moderate 5%–25%; Minor <5%; [2] CFA = carbonate-fluorapatite; Px = pyroxene; ASi = amorphous silica; 10 Å manganate = todorokite, buserite, or asbolane; [3] Sample treated with 0.5 M triammonium citrate and 30% H_2O_2; – means not present; (?) means presence uncertain; NA means not available.

X-ray diffraction mineralogy on all samples was completed using a Philips diffractometer (Philips, Amsterdam, The Netherlands) with Cu Kα radiation and graphite monochromator. Semi-quantitative mineral percentages were calculated by using peak intensities and weighting factors relative to quartz set as 1 [14,15]. The detection limit for each mineral falls between about 0.2% and 1.0%.

Chemical analyses of major and minor elements for all samples were done at SGS analytical laboratory, Canada. The concentrations of the 10 major elements were determined by XRF on a borate-fused disk; Ba, Cr, Cu, Li, Ni, S, Sr, V, Zn, and Zr by ICP using four-acid (HCl, HF, HNO_3, and $HClO_4$) digest, with resulting solutions dried and then dissolved in 1 mL of aqua regia and diluted to 10.0 g with 1% HNO_3; Ag, As, Be, Bi, Cd, Cs, Ga, Hf, In, Mo, Pb, Rb, Sb, Sc, Se, Sn, Ta, Te, Tl, and

W by ICP-mass spectrometry (ICP-MS) after the same four-acid digest procedure; Co, Nb, Th, U, V, Zr, and REY by ICP-MS using a Li-metaborate fused disk that was dissolved in weak HNO_3; CO_2 by combustion and infrared spectroscopy; and F and Cl by specific-ion electrode. For leached phosphorite samples only, CO_2 concentrations were determined by coulometric titration, and S by combustion and infrared spectroscopy. The Pearson correlation coefficient was used to calculate coefficient matrices for the chemical data.

REY plots were normalized to shale (PAAS, Post-Archean Australian Shale [16]). The Ce anomaly was calculated as $Ce^* = Ce_N/Pr_N$ with both PAAS- and chondrite-normalized [17] values; $Ce^* = 2Ce_N/La_N + Pr_N$ was not used because of the strong positive La anomaly (see [18]).

3. Results

This study provides data for high-grade phosphorite deposits from the various global-ocean settings described in the Samples and Methods section. Phosphatization forms a continuum from pervasive, which produces nearly pure CFA rocks, to rocks showing only minor phosphatization and detrital minerals or biogenic carbonates dominate (Figure 3). Many bulk untreated phosphorite samples contain only CFA, as do the leached samples (Tables 1 and 2).

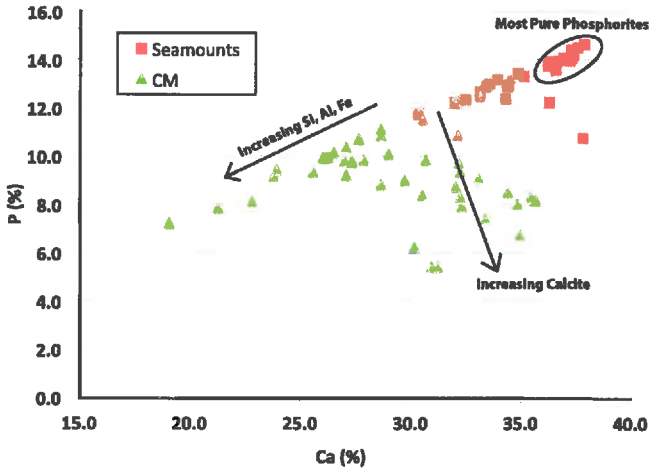

Figure 3. Scatter plot of phosphorus versus calcium for seamount and continental margin phosphorite deposits analyzed here. Arrows show deviations from the carbonate fluorapatite end member (most pure phosphorite) with increasing calcite and detrital/authigenic (Si, Al, and Fe) contents.

3.1. Mineralogy

The seamount phosphorites are composed predominantly of CFA, with lesser amounts of biogenic calcite, and detrital quartz and feldspars (Table 1); other minor to trace minerals are also present. The seamount samples selected for leaching were composed predominantly of CFA and calcite. Once leached, 13 of the 17 contained only CFA, two also contained phillipsite, and two have minor quartz (Table 1). The mineralogy of the CM phosphorites varies with location. The California borderland phosphorites are the most pure, with minor detrital and authigenic mineral fractions in 60% of the samples and moderate amounts of detrital minerals in 40% of the samples (Table 2). Chatham Rise and Black Plateau samples are the most carbonate-rich phosphorites, with calcite being a major phase in several samples. Detrital minerals and authigenic glauconite are also common in phosphorites from those two areas. The Peru margin phosphorites contain the highest detrital and authigenic mineral fractions (Table 2).

3.2. Geochemistry

The chemical composition supports the XRD mineralogy and shows that all samples are composed predominantly of CFA, based on P contents. The Ca content is distributed among the CFA, biogenic carbonate, and detrital minerals. The Ca/P ratios indicate that more calcite occurs in Chatham Rise and Blake Plateau phosphorites (3.7 and 3.6 respectively; Tables 3–8, Table S1; Figure 3) compared to the other CM and seamount phosphorites (2.6 to 2.7), especially the Blake Plateau samples, which also have the lowest mean Ca/CO_2 ratio (2.45). Si and Al contents increase with increasing contents of biogenic silica, authigenic quartz, and detrital quartz and aluminosilicate minerals. Peru margin phosphorites have the highest aluminosilicate fraction and the seamount phosphorites the lowest, which is consistent with distance from detrital sources. Seamount phosphorites have Si/Al ratios (mean 3.0; 2.9 leached) similar to mean MORB and mean ocean crust (2.9–3.1), whereas all the CM deposits have Si/Al ratios (3.9–4.2) similar to upper continental crust (3.8–4.2), except Chatham Rise phosphorites (7.4). The Chatham Rise phosphorites show excess silica over typical continental detrital ratios, which reflect either biogenic silica (diatoms) or abundant quartz, the former being most likely. In general, Peru margin, Chatham Rise, and Blake Plateau phosphorite samples contain the highest non-phosphate components, predominantly detrital aluminosilicates, biogenic silica, and biogenic calcite respectively.

Table 3. Statistics of phosphorite deposits from the California Borderland (see Table S1 for full dataset).

Element	*N*	Mean [1]	Median	StDev	Min	Max
Fe (wt %)	10	1.60	1.37	0.90	0.50	3.27
Si	10	3.73	2.58	2.80	0.73	9.07
Al	10	0.95	0.61	0.94	0.16	3.01
Si/Al	10	3.94	5.12	1.36	2.68	6.24
Mg	10	0.71	0.57	0.33	0.43	1.36
Ca	10	30.6	32.1	3.83	22.8	34.5
Na	10	1.27	1.18	0.27	1.02	1.85
K	10	0.41	0.44	0.19	0.15	0.72
Ti	10	0.19	0.03	0.33	0.01	0.89
P	10	11.6	12.3	1.67	8.16	13.2
Ca/P	10	2.64	2.63	0.07	2.57	2.79
P_2O_5	10	26.6	28.1	3.84	18.7	30.3
S	10	1.10	1.13	0.28	0.62	1.58
SO_3	10	2.74	2.81	0.69	1.55	3.93
CO_2	10	6.31	6.60	0.93	4.34	7.06
LOI [2]	10	11.1	11.0	0.69	10.2	12.2
H_2O^+	10	4.71	4.75	0.23	4.40	5.05
As (ppm)	10	13	13	6.1	6.0	27
Ba	10	684	647	487	145	1290
Cl	10	1032	905	368	670	1790
Co	10	5.8	4.3	3.5	2.8	13
Cr	10	111	107	45	43	181
Cu	10	23	20	5.0	18	31
F	10	20,909	22,750	5205	8990	25,400
Li	10	6.4	4.5	5.7	2.0	20
Mn	10	79	33	91	17	256
Mo	10	10	6.7	12	4.0	44
Ni	10	44	43	6.0	35	55
Pb	10	4.2	3.6	1.7	2.2	7.6
Sr	10	2072	2100	257	1560	2340
U	10	106	83	67	62	285
V	10	101	115	41	49	165
Zn	10	57	49	19	41	94
Zr	10	37	16	46	8.0	141
La	10	23.6	23.0	6.37	15.1	32.6

Table 3. *Cont.*

Element	*N*	Mean [1]	Median	StDev	Min	Max
Ce	10	18.7	14.7	11.5	7.00	42.6
Pr	10	4.23	3.77	1.78	2.05	7.39
Nd	10	16.8	15.0	7.08	7.90	29.4
Sm	10	3.43	3.03	1.50	1.60	6.10
Eu	10	0.97	0.82	0.48	0.43	1.85
Gd	10	4.63	4.49	1.49	2.48	6.53
Tb	10	0.71	0.70	0.22	0.38	1.00
Dy	10	4.61	4.66	1.29	2.63	6.34
Y	10	59.7	59.7	13.4	40.2	78.4
Ho	10	1.07	1.10	0.26	0.67	1.44
Er	10	3.51	3.54	0.82	2.25	4.55
Tm	10	0.49	0.50	0.11	0.31	0.63
Yb	10	2.79	2.85	0.56	1.90	3.60
Lu	10	0.43	0.43	0.09	0.30	0.58
ΣREY [3]	10	146	144	41	85	205
%HREY [4]	10	54	57	6	42	61
Ce_{cn} [5]	10	0.63	0.62	0.14	0.38	0.85
Ce_{sn} [5]	10	0.47	0.47	0.10	0.29	0.64

[1] Mean, Median, Min, Max in wt % (Fe to As) and ppm (As and below); [2] %Loss on ignition at 1000 °C; H_2O^+ is structural water; [3] ΣREY = Sum of rare earth elements plus yttrium; [4] %HREY (Eu–Lu) of the total sum of REY; [5] Ce_{cn} = Ce anomaly using chondrite-normalized values; Ce_{sn} = Ce anomaly using PAAS-normalized values.

Table 4. Statistics of phosphorite deposits from Peru Margin.

Element	*N*	Mean [1]	Median	StDev	Min	Max
Fe (wt %)	10	1.72	1.55	0.60	1.17	2.97
Si	10	8.47	7.41	3.08	5.05	14.6
Al	10	2.00	1.68	0.66	1.34	3.31
Si/Al	10	4.23	4.10	0.50	3.51	4.87
Mg	10	0.66	0.67	0.09	0.42	0.74
Ca	10	25.2	26.3	3.09	19.1	28.7
Na	10	1.31	1.26	0.17	1.05	1.60
K	10	0.73	0.65	0.26	0.44	1.21
Ti	10	0.09	0.08	0.02	0.07	0.13
P	10	9.69	10.1	1.27	7.24	11.1
Ca/P	10	2.60	2.60	0.04	2.53	2.70
P_2O_5	10	22.2	23.1	2.91	16.6	25.5
S	10	1.40	1.37	0.54	0.73	2.63
SO_3	10	3.50	3.42	1.35	1.82	6.55
CO_2	10	5.90	6.22	1.01	4.03	7.02
LOI [2]	10	10.6	10.8	1.50	8.07	13.3
H_2O^+	10	4.49	4.55	0.66	3.50	5.40
As (ppm)	10	29	26	20	7.0	81
Ba	10	136	106	64	84	281
Cl	10	1829	1762	595	1007	3037
Co	10	3.9	4.0	1.0	2.7	5.5
Cr	10	76	70	23	49	116
Cu	10	13	14	2.2	8.4	15
F	10	22,157	20,588	3747	18173	29,394
Li	10	10	11	2.0	7.0	14
Mn	10	98	91	21	71	141
Mo	10	17	12	17	2.9	63
Ni	10	43	42	18	21	81
Pb	10	6.4	6.0	1.8	4.2	9.8

Table 4. *Cont.*

Element	*N*	Mean [1]	Median	StDev	Min	Max
Sr	10	1756	1855	238	1330	1980
U	10	115	123	35	48	177
V	10	62	64	12	40	80
Zn	10	40	40	8.3	30	56
Zr	10	71	75	22	36	95
La	10	10.4	10.5	1.25	8.50	12.6
Ce	10	17.7	16.8	2.98	14.7	23.5
Pr	10	2.30	2.22	0.32	1.96	2.93
Nd	10	9.09	9.20	1.18	7.50	11.1
Sm	10	1.84	1.85	0.26	1.50	2.20
Eu	10	0.47	0.46	0.09	0.33	0.62
Gd	10	2.00	2.09	0.31	1.41	2.46
Tb	10	0.31	0.31	0.04	0.24	0.37
Dy	10	1.96	1.98	0.35	1.27	2.39
Y	10	18.8	18.4	4.39	9.60	24.2
Ho	10	0.44	0.44	0.08	0.28	0.54
Er	10	1.33	1.34	0.24	0.83	1.70
Tm	10	0.21	0.21	0.04	0.12	0.25
Yb	10	1.32	1.33	0.22	0.80	1.60
Lu	10	0.22	0.22	0.04	0.12	0.27
ΣREY [3]	10	68	70	9	52	80
%HREY [4]	10	40	41	5	29	45
Ce_{cn} [5]	10	1.13	1.12	0.04	1.07	1.19
Ce_{sn} [5]	10	0.85	0.84	0.03	0.81	0.90

See Table 3 for footnotes.

Table 5. Statistics of phosphorite deposits from Chatham Rise.

Element	*N*	Mean [1]	Median	StDev	Min	Max
Fe (wt %)	15	3.24	3.08	1.23	1.26	5.00
Si	15	4.28	4.62	1.91	1.33	6.55
Al	15	0.58	0.60	0.31	0.17	1.39
Si/Al	15	7.41	7.65	1.95	3.93	11.4
Mg	15	0.62	0.59	0.22	0.34	0.93
Ca	15	31.0	30.9	3.08	27.0	35.7
Na	15	0.70	0.69	0.04	0.63	0.78
K	15	1.05	1.01	0.59	0.33	1.92
Ti	15	<0.04	<0.01	0.09	<0.01	0.31
P	15	8.36	8.77	1.50	5.45	9.86
Ca/P	15	3.72	3.65	0.99	2.75	5.73
P_2O_5	15	19.2	20.1	3.43	12.5	22.6
S	15	0.64	0.64	0.12	0.47	0.90
SO_3	15	1.59	1.60	0.29	1.17	2.25
CO_2	2	5.82	5.82	0.43	5.51	6.12
LOI [2]	15	16.9	16.8	5.22	9.97	24.2
H_2O^+	2	4.05	4.05	0.07	4.00	4.10
As (ppm)	15	22	23	7.9	11	39
Ba	15	94	50	91	34	335
Cl	15	850	810	346	340	1630
Co	15	6.7	7.7	2.1	3.0	9.7
Cr	15	40	44	20	15	76
Cu	15	8.0	7.0	4.5	1.0	17
F	15	17,860	17,400	4085	11,000	24,800
Li	15	7.7	8.0	3.6	3.0	13

Table 5. *Cont.*

Element	*N*	Mean [1]	Median	StDev	Min	Max
Mn	15	93	78	65	57	324
Mo	15	2.9	2.8	1.5	0.94	7.3
Ni	15	30	30	10	15	53
Pb	15	12	12	4.7	5.2	20
Sr	15	1447	1330	493	1110	2660
U	15	155	130	77	64	334
V	15	71	73	16	47	94
Zn	15	27	27	5.4	17	38
Zr	15	24	22	9.7	10	52
La	15	22.7	20.4	13.6	7.60	48.9
Ce	15	15.6	15.8	8.05	4.10	29.8
Pr	15	2.84	2.75	1.35	1.02	5.38
Nd	15	11.5	11.2	5.41	4.30	21.7
Sm	15	1.97	1.90	0.86	0.80	3.60
Eu	15	0.49	0.47	0.22	0.18	0.90
Gd	15	2.71	2.52	1.27	1.09	5.11
Tb	15	0.39	0.36	0.18	0.16	0.73
Dy	15	2.54	2.32	1.21	0.98	4.88
Y	15	37.6	33.8	21.0	13.6	78.1
Ho	15	0.67	0.61	0.34	0.25	1.35
Er	15	2.04	1.84	1.01	0.82	4.09
Tm	15	0.29	0.26	0.14	0.12	0.57
Yb	15	1.75	1.60	0.84	0.70	3.40
Lu	15	0.26	0.22	0.13	0.10	0.53
ΣREY [3]	15	103	95	55	36	209
%HREY [4]	15	47	48	3	38	50
Ce_{cn} [5]	15	0.78	0.81	0.08	0.59	0.87
Ce_{sn} [5]	15	0.59	0.61	0.06	0.45	0.66

See Table 3 for footnotes.

Table 6. Statistics of phosphorite deposits from Blake Plateau.

Element	*N*	Mean [1]	Median	StDev	Min	Max
Fe (wt %)	10	2.35	2.34	1.12	0.80	3.88
Si	10	2.86	2.42	1.51	1.17	6.45
Al	10	0.71	0.75	0.28	0.31	1.28
Si/Al	10	4.04	4.35	2.15	1.60	7.91
Mg	10	0.65	0.64	0.16	0.43	0.92
Ca	10	31.8	32.2	2.07	27.1	34.9
Na	10	0.71	0.70	0.12	0.53	0.91
K	10	0.51	0.50	0.33	0.19	1.27
Ti	10	0.05	0.04	0.03	0.02	0.11
P	10	8.80	8.84	1.25	6.76	10.9
Ca/P	10	3.61	3.53	0.72	2.93	5.17
P_2O_5	10	20.2	20.3	2.86	15.5	25.0
S	10	0.68	0.66	0.14	0.51	0.96
SO_3	10	1.70	1.64	0.35	1.27	2.40
CO_2	10	13.0	12.9	4.01	6.62	20.0
LOI [2]	10	16.7	16.4	3.84	11.3	23.8
H_2O^+	10	3.70	3.90	0.70	2.45	4.50
As (ppm)	10	35	34	15	12	59
Ba	10	323	217	394	22	1301
Cl	10	506	457	202	199	895
Co	10	126	56	137	5.6	338

Table 6. *Cont.*

Element	*N*	Mean [1]	Median	StDev	Min	Max
Cr	10	99	82	92	12	269
Cu	10	72	17	95	5.4	290
F	10	27,216	27,516	3248	21,912	32,171
Li	10	14	12	7.7	7.0	31
Mn	10	9108	4647	11,565	232	30,051
Mo	10	22	13	22	3.5	72
Ni	10	467	107	583	26	1738
Pb	10	19	13	14	4.9	40
Sr	10	1376	1354	300	1001	1990
U	10	62	36	84	5.3	285
V	10	113	122	39	37	174
Zn	10	87	93	41	39	160
Zr	10	73	79	43	22	151
La	10	71.1	57.9	42.5	23.4	133
Ce	10	36.2	34.4	20.7	7.60	77.8
Pr	10	10.8	8.48	6.73	3.83	22.6
Nd	10	48.0	37.1	30.6	17.0	102
Sm	10	9.09	7.10	5.93	3.10	20.1
Eu	10	2.45	1.93	1.57	0.88	5.23
Gd	10	12.9	10.1	8.43	4.48	27.1
Tb	10	1.71	1.32	1.10	0.61	3.53
Dy	10	11.8	8.92	7.60	4.17	23.1
Y	10	130	101	83.7	38.4	257
Ho	10	2.58	1.97	1.66	0.87	4.76
Er	10	7.75	5.80	4.97	2.55	14.8
Tm	10	1.17	0.88	0.75	0.38	2.32
Yb	10	6.65	4.90	4.36	2.20	13.9
Lu	10	1.19	0.87	0.79	0.38	2.52
ΣREY [3]	10	353	286	211	124	663
%HREY [4]	10	50	51	7	33	59
Ce_{cn} [5]	10	0.55	0.50	0.29	0.27	1.24
Ce_{sn} [5]	10	0.41	0.38	0.22	0.20	0.94

See Table 3 for footnotes.

Table 7. Statistics of unleached phosphorite deposits from seamounts.

Element	*N*	Mean [1]	Median	StDev	Min	Max
Fe (wt %)	12	0.66	0.42	0.75	0.06	2.89
Si	12	2.33	1.86	2.11	0.03	7.15
Al	12	0.78	0.64	0.65	0.02	2.12
Si/Al	12	2.99	2.87	0.52	1.55	3.37
Mg	12	0.27	0.24	0.14	0.11	0.62
Ca	12	34.7	35.4	3.25	26.2	37.8
Na	12	0.80	0.83	0.15	0.56	1.09
K	12	0.36	0.27	0.31	0.02	0.86
Ti	12	<0.08	<0.05	0.08	<0.01	0.28
P	12	12.7	12.9	1.27	9.95	14.0
Ca/P	12	2.73	2.66	0.26	2.58	3.51
P_2O_5	12	29.1	29.7	2.90	22.8	32.2
S	12	0.68	0.71	0.09	0.54	0.80
SO_3	12	1.71	1.76	0.22	1.35	2.00
CO_2	9	5.12	5.13	1.22	3.75	6.96
LOI [2]	12	9.14	8.08	2.90	6.67	17.5
H_2O^+	9	2.22	2.10	0.32	1.90	2.80
As (ppm)	12	5.2	5.0	1.7	3.0	9.0

Table 7. *Cont.*

Element	N	Mean [1]	Median	StDev	Min	Max
Ba	12	483	81	725	20	1900
Cl	12	1208	755	958	310	3410
Co	12	21	12	22	1.7	67.8
Cr	12	21	14	15	7.0	51.0
Cu	12	77	64	56	15	205
F	12	25,767	28,250	5461	12,300	30,300
Li	12	<6.6	<6.0	5.9	<1.0	20
Mn	12	1210	775	1343	46	3873
Mo	12	3.1	2.8	2.3	0.75	7.3
Ni	12	116	61	115	21	366
Pb	12	7.0	6.3	5.1	1.1	15
Sr	12	1223	1175	338	724	1920
U	12	6.7	6.3	1.9	4.7	11
V	12	33	33	10	22	59
Zn	12	51	49	20	26	100
Zr	12	91	79	52	9.5	211
La	12	102	79.7	61.8	16.6	214
Ce	12	15.0	13.1	7.56	3.10	30.2
Pr	12	14.4	9.21	10.3	2.85	36.8
Nd	12	60.6	38.8	43.6	11.9	153
Sm	12	11.5	7.05	8.82	2.40	31.1
Eu	12	3.26	2.16	2.43	0.73	8.31
Gd	12	18.2	13.2	12.8	3.47	42.5
Tb	12	2.44	1.87	1.65	0.46	5.67
Dy	12	17.4	14.5	11.3	3.03	38.7
Y	12	224	205	132	38.9	437
Ho	12	4.19	3.75	2.54	0.71	8.69
Er	12	13.4	12.3	7.88	2.29	26.9
Tm	12	1.88	1.77	1.10	0.34	3.88
Yb	12	12.9	12.3	7.62	2.40	27.2
Lu	12	1.98	1.92	1.19	0.35	4.19
ΣREY [3]	12	503	434	292	112	1022
%HREY [4]	12	60	58	8	47	74
Ce_{cn} [5]	12	0.25	0.17	0.34	0.06	1.29
Ce_{sn} [5]	12	0.19	0.13	0.25	0.05	0.98

See Table 3 for footnotes.

Table 8. Statistics of leached phosphorite deposits from seamounts [a].

Element	N	Mean [1]	Median	StDev	Min	Max
Fe (wt %)	18	0.46	0.39	0.39	0.01	1.38
Si	18	1.67	1.26	1.44	0.32	5.28
Al	18	0.58	0.43	0.54	0.05	1.88
Si/Al	18	2.88	3.13	1.10	2.19	6.01
Mg	18	0.21	0.20	0.11	0.04	0.45
Ca	18	35.4	36.3	2.08	30.4	37.9
Na	18	0.66	0.66	0.11	0.50	0.85
K	18	<0.17	<0.06	0.19	<0.01	0.69
Ti	18	<0.05	<0.04	0.05	0.004	0.22
P	18	13.5	13.8	0.84	11.8	14.6
Ca/P	18	2.62	2.63	0.04	2.58	2.77
P_2O_5	18	31.0	31.6	1.93	27.0	33.5
S	18	0.71	0.72	0.15	0.49	0.94
SO_3	18	1.77	1.79	0.37	1.22	2.35
CO_2	18	6.35	6.40	1.35	3.84	7.99
LOI [2]	18	8.73	8.58	1.44	5.88	11.7

Table 8. *Cont.*

Element	*N*	Mean [1]	Median	StDev	Min	Max
H_2O^+	5	2.14	2.34	0.33	1.76	2.45
As (ppm) [b]	0	--	--	--	--	--
Ba	13	4401	267	521	195	2140
Cl	18	497	400	646	50	2980
Co	13	11	10	5.3	4.0	23
Cr	13	18	18	7.1	9.0	33
Cu	15	38	34	20	15	89
F	18	39,011	39,250	4078	31,800	46,000
Li	13	5.5	5.0	2.7	2.0	10
Mn	18	709	300	1550	75	6816
Mo	12	5.5	5.5	2.2	1.0	9.0
Ni	13	23	21	15	9.0	71
Pb	13	151	146	41	91	218
Sr	15	1563	1410	453	1000	2580
U	16	12	8.5	7.3	6.3	30
V	13	35	35	10	21	50
Zn	13	80	63	49	38	205
Zr	13	44	38	18	20	77
La	18	180	189	89.2	7.20	372
Ce	18	28.5	29.4	17.9	2.00	74.0
Pr	18	23.1	20.0	13.7	1.00	49.3
Nd	18	102	88.9	60.2	4.40	222
Sm	18	20.3	17.3	12.9	0.97	46.8
Eu	18	5.33	4.77	3.21	0.22	11.8
Gd	18	32.2	29.9	19.1	1.40	73.9
Tb	18	4.69	4.45	2.80	0.18	10.7
Dy	18	30.8	29.6	17.8	1.40	69.7
Y	13	441	415	233	145	976
Ho	18	8.16	8.38	4.64	0.41	19.2
Er	18	24.6	25.3	13.8	1.20	57.3
Tm	18	3.51	3.50	1.99	0.20	8.30
Yb	18	21.7	20.8	12.4	1.30	52.2
Lu	13	3.74	3.41	2.00	1.03	8.01
ΣREY [3]	13	935	824	490	250	1992
%HREY [4]	13	62	62	5	56	70
Ce_{cn} [5]	18	0.20	0.19	0.08	0.05	0.35
Ce_{sn} [5]	18	0.15	0.14	0.06	0.04	0.27

[a] Samples treated with 0.5 M triammonium citrate and 30% H_2O_2; [b] – = data not analyzed; See Table 3 for other footnotes.

3.3. *Rare Earth Elements (REY)*

The continental-margin deposits have relatively low grades, with average total REY of 161 ppm (68–353 ppm, maximum 663 ppm; Tables 3–8, Table S2). Grades for the seamount phosphorite deposits are higher, averaging 727 ppm total REY (maximum 1992 ppm; Tables 7 and 8, Table S3). However, the most interesting characteristic of both groups of phosphorites is the high percentages of the HREY. For the CM deposits, the %HREY ranges from 29% to 61% and averages 49%. For the seamount group, the average %HREY is 60% (range 47%–74%). The highest values come from the equatorial west Pacific seamounts (60%–74% HREY complement).

The Pacific and northeast Atlantic CM REY datasets are similar and differ significantly from the Blake Plateau dataset (Tables 3–6). The Blake samples have the highest Mn concentration, which increases the concentrations of the Mn-hosted metals, such as Co, Ni, V, Pb, Zn, Zr, Cu, Mo, and REY. Consequently, Blake Plateau phosphorites have the highest REY contents compared to the other CM deposits, mean 353 ppm.

The highest concentrations of individual REY in all deposits are Y, La, and Nd in decreasing order, with Y significantly enriched over the others (Figure 4). The seamount phosphorites are enriched in all the REY except Ce compared to the CM phosphorites. The Blake Plateau and NE Atlantic datasets have the highest Ce contents. Besides Y, other HREY are significantly enriched in the seamount samples, Gd, Dy, Er, and Yb (Figure 4). Plots of PAAS-normalized REY show HREY enrichments relative to LREY, negative Ce anomalies (Ce *), and positive Y, Gd, and La anomalies (Figure 5). These characteristics generally reflect those of seawater, but the Ce * varies widely. Ce * increases in magnitude with increasing total REY contents, so the Peru margin and seamount phosphorites have the smallest and largest magnitude anomalies, respectively, compared to the other datasets.

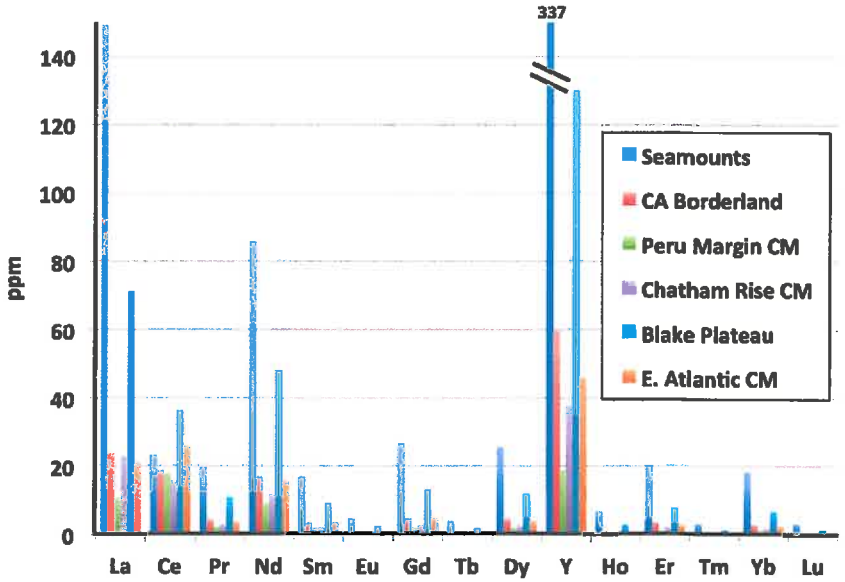

Figure 4. Bar diagram of mean contents of individual rare earth elements and yttrium for the sample groups studied here; note that the order for each element follows the order in the key.

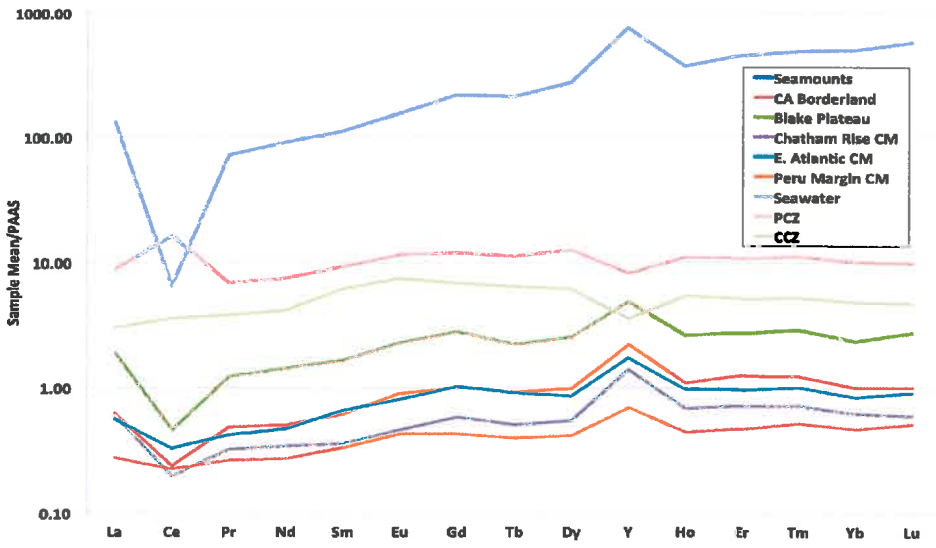

Figure 5. Post Archean Australian Shale-normalized rare earth element plot for mean data of sample groups compared with patterns for Prime Crust Zone (PCZ) crusts, Clarion-Clipperton Zone (CCZ) nodules, and seawater ($\times 10^9$) at ~2000 m water depth [19].

3.4. Correlations

The presence of calcite and Mn oxides in the CM phosphorites changes the correlation coefficients for the CFA-hosted elements. The California and Peru margin samples have the lowest calcite and/or Fe-Mn oxides and show positive correlations among Ca, P, Sr, S, CO_2, and %HREY, and at a lower statistical significance (95% confidence level: CL) with F, Cl, Mg, Sb, Cd, Mo, Se, U, Tl, and Ag. These elements can be considered to be associated for the most part with the CFA. The REY are fractionated among the CFA, aluminosilicate, and Mn-oxide minerals. With higher calcite contents, Ca no longer correlates with the other CFA elements (except CO_2) at the 95% CL and has either a negative correlation with total REY (Chatham samples) or no correlation with total REY (Blake samples). ΣREY correlates at the 95%–99% CL predominantly with Mn and Fe-Mn-oxide associated elements in Blake samples. Mn in Blake samples correlates with Co, Ni, ΣREY, each REY (except Ce), Cu, Ti, Mo, Tl, W, Cd, Li, and Sc; coefficients are higher for the HREY than for the LREY.

The seamount samples show positive correlations among Ca, P, S, CO_2, Na, F, Sr, U, and %HREY. These elements are considered to be associated with the CFA and as that phase increases so does the content of HREY. The REY are distributed among the CFA, Mn oxides, and aluminosilicate minerals. The elements that typically correlate with Si and Al in all the datasets are Fe, Na, K, Rb, Mg, Ti, Zr, Be, Cd, Th, Nb, and the LREY, which make up the silicate fraction of the phosphorites.

4. Discussion

4.1. Comparison of CM and Seamount Mineralization, and REY Mass Balance

It is well known that apatite is a key mineral in the acquisition of REY from a wide variety of fluids occurring in many different geological settings (e.g., [20,21]). Our data show that CM marine phosphorites have relatively low total REY concentrations with high complements of HREY. In comparison, seamount phosphorites have about four to six times higher individual REY concentrations than CM phosphorites, except for Ce, which is comparable, and very high HREY complements. The seamount deposits generally have lower detrital (mean 9.4% versus 12.1% for CM), biosilica, and biocalcite contents and consequently higher Ca and P contents, forming more pure CFA (mean 72% CFA) seamount phosphorite deposits compared to CM deposits (mean 54% CFA), based on formulas to calculate normative components from [22]. However, the higher Ca and P contents are only part of the story and do not fully explain the higher REY concentrations and higher complement of HREY in the seamount deposits. Based on mass-balance calculations, a small part of the REY content (8% for CM, 2% for seamount deposits) occurs in the detrital/authigenic mineral fraction and the remainder is associated with the CFA, and also minor concentrations with the Fe-Mn oxides in Blake Plateau samples and with calcite in samples from all areas. This is further reflected in the seamount phosphorite samples, which have the lowest detrital and authigenic fractions and the highest REY contents.

4.2. CFA Structure and Substitutions by REY

The REY typically exchange for Ca in the CFA structure; the LREY favor the Ca2 structural site and the HREY the Ca1 structural site, with the REY near Eu in ionic radius having no preference (e.g., [21]). Charge balance has to be maintained for substitutions in the CFA structure as there are many elements that can substitute for the Ca^{2+} and PO_4^{3-}. Substitution of the trivalent REY for divalent Ca produces a charge imbalance that can be offset for example by the substitution of monovalent Na for Ca, silicate for phosphate, or charge-balancing anions such as F and Cl.

For the non-calcite bearing samples, the Ca/P ratios and CO_2 contents are about the same for seamount and CM deposits, but Ca/CO_2, P/CO_2, Ca/Na, P/Na, and the magnitude of the negative Ce * are much lower for the CM phosphorites. These and other ratios indicate that there is comparatively less CO_2, SO_3, and Na relative to the main structural elements in the CFA of seamount phosphorites. The seamount CFA has more F and less Cl and Sr than the mean for the CFA fraction of

the CM phosphorites. Of these relationships, less CO_2 (CO_3) and SO_3 substitution for PO_4, and higher F would aid in the charge balance created by the substitution of trivalent elements for the divalent Ca in the seamount CFA relative to the CM CFA. Although they can explain some variance, these chemical differences also cannot fully explain the different REY contents and LREY/HREY fractionations in CM versus seamount phosphorites.

4.3. Controls on REY Composition

There are four fundamental differences between the CM and seamount phosphorites. The seamount phosphorites are older and have therefore had more time for aging that might have allowed for greater REY adsorption, substitution, and replacement in the CFA. A second difference is the generally greater water depth of formation of the seamount phosphorites (1000 to ~3000 m) compared to CM deposits (10s to 100s m). The Pacific Cretaceous seamounts had subsided to near their present depths by the time the Paleogene and Miocene phosphorites had formed [4]. Dissolved REY, except Ce, increase with increasing water depth in the open Pacific Ocean (e.g., [23,24]), which would offer a greater REY reservoir to tap during formation of deep-water phosphorites. The increases of the REY with water depth are significant, 5–10 times increases from the sea surface to 3000 m water depth, the variation depending on the individual REY and location in the global ocean (e.g., [24]). A corollary to this is that the seamount phosphorites formed earlier in the Cenozoic [4], when environmental conditions favored greater supplies of REY from seawater (e.g., [25]), and perhaps slower rates of precipitation of Fe-Mn oxyhydroxides due to intensified suboxic conditions (e.g., [10]). A difficulty in applying inferences from the geological record is that most of the deposits analyzed formed at continental margins and REY concentrations at various water depths through time in open-ocean environments are not as well known.

The association of seamount phosphorites with Fe-Mn oxides is the third fundamental difference with CM phosphorites. However, both groups of phosphorites obtain REY from seawater, which has a REY pattern controlled by complex processes, including the sorption of REY on Fe-Mn oxides and other materials, release of REY from dissolving bio-silica (opal) and bio-calcite, and solution complexation dominated by mono- and di-carbonate complexes [18,23–25]. These processes are also water-depth dependent, as with the distribution of REY concentrations, indicating a significant water-depth impact on REY incorporation into the phosphorites. In addition, CM phosphorites obtain REY from pore fluids influenced by diagenetic reactions. Both groups of phosphorites also inherit a small amount of their REY complements from the carbonates that were replaced (e.g., [2]).

The Fe-Mn crusts and phosphorites obtain REY from seawater by different mechanisms, crusts by sorption of the REY and oxidation of the Ce, and phosphorites by substitution for Ca during precipitation, and to lesser extents by inheritance and sorption. Seamount phosphorite mean REY contents normalized to mean Prime Crust Zone (PCZ [26]) Fe-Mn crusts show a very large positive Y anomaly, a smaller positive La anomaly, and smaller yet positive Gd anomaly, as well as a large negative Ce anomaly; this ratio generally increases with increasing atomic number (Figure 6). These anomalies are opposite to the anomalies found for Fe-Mn crusts but are the same anomalies found for seawater [18]. Seawater, Fe-Mn crusts, and phosphorites are HREY enriched relative to LREE, but to different degrees, with seawater at ~2000 m water depth in the central Pacific showing 73% HREY complement of total REY [19] versus a mean of 60% (range 47%–74%) for seamount phosphorites and mean of 18% for PCZ Fe-Mn crusts [27]. The seamount phosphorite REY pattern compares closely with that of intermediate depth seawater in the central Pacific. If crust growth slowed or even stopped during phosphatization of the crusts and substrate rocks, it is possible that this process changed the LREY/HREY ratio and REY concentrations of seawater from which the seamount phosphorites precipitated over million-year time frames. The range of that ratio for the seamount phosphorites is consistent with that idea, but necessary data are not available to verify it.

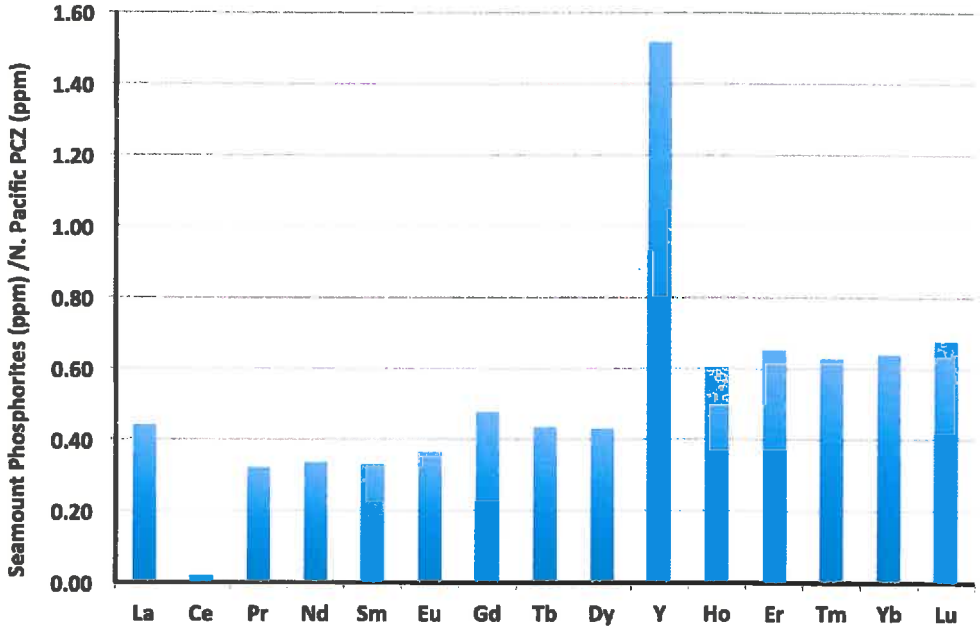

Figure 6. Bar diagram of ratio of mean REY data for seamount phosphorites and Pacific Prime Crust Zone ferromanganese crusts.

A fourth major difference is that phosphatization of the seamount deposits occurred in an organic-matter-poor sedimentary environment (e.g., [28]), which did not allow for redox diagenetic zones to be established in the sediment that was cemented and replaced by the CFA. Seamount foraminiferal sands, the most commonly replaced sediment type, and reef limestone [29], have pore waters that are the same as seawater, which during phosphatization were likely suboxic; the upper meters of sediment/limestone act as an open system. In contrast, most CM deposits formed in organic matter-rich environments that promoted complex diagenetic zones that changed as sediment was eroded and deposited. Many chemical reactions in different diagenetic zones, such as Mn and Fe reduction, organic matter oxidation, suboxic diagenesis, anoxic sulfate reduction, methanogenesis, etc., promoted the formation of different authigenic minerals, such as glauconite, pyrite, dolomite, and other metal carbonates (e.g., [11,12,30], and references therein). These diagenetic processes may in part fractionate the REY among the authigenic phases, including the CFA in phosphorite; the diagenetic fluid that contributes to the formation of the phosphorite is less enriched in REY compared to seawater unaltered by these diagenetic reactions.

4.4. Comparisons with Terrestrial Carbonatite REY Deposits and Marine Fe-Mn Deposits

These marine phosphorites contrast with the typical, large, land-based carbonatite-hosted REY, which have a HREY complement of <1%, and very high grades for the LREY [31]. Carbonatites are the deposits from which more than 90% of the REY used by industry are produced. The existing, and soon to be operational, carbonatite-hosted REY deposits can supply the LREY needed by industry, but not the HREY.

Marine Fe-Mn crusts and nodules, which are considered as potential resources for REY, especially the HREY, also have on average much lower HREY complements than the phosphorites, mean 17% for crusts and 22% for nodules (Figure 7); but crusts have total REY grades up to 1%, but more typically 0.20% to 0.40%, while nodules have lower grades, 0.08% for Clarion-Clipperton Zone (CCZ) and 0.17% for Cook island nodules (Figure 8) [27,32–34]. As mentioned, it is the HREY complement that is most important because those elements are most needed for high-tech and green-tech applications and have

the highest per weight market value (e.g., LCDs, permanent magnets, solar panels, lasers, nuclear medicine, phosphors) [35].

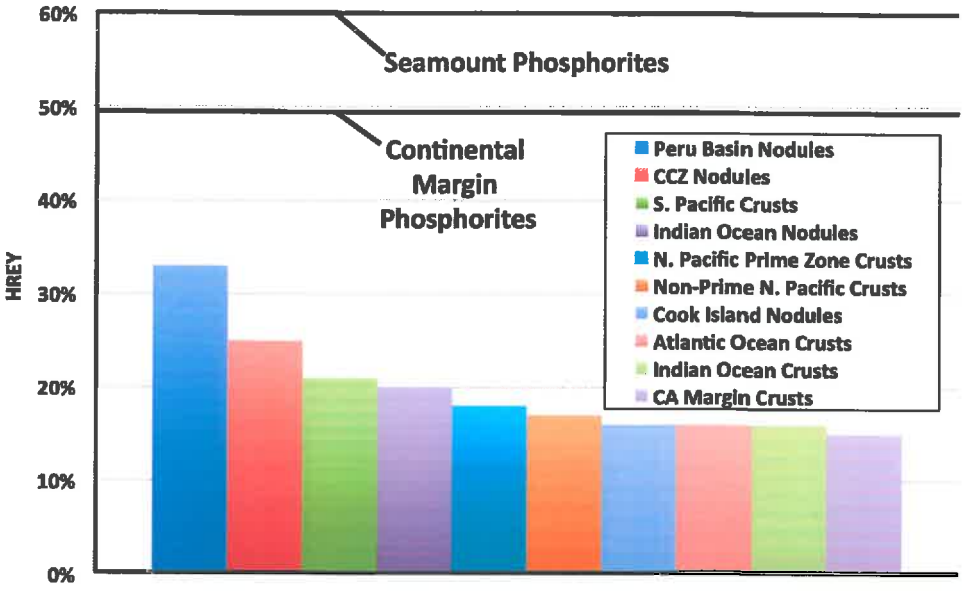

Figure 7. Comparison of mean total HREY contents of ferromanganese deposits with seamount and continental margin phosphorites.

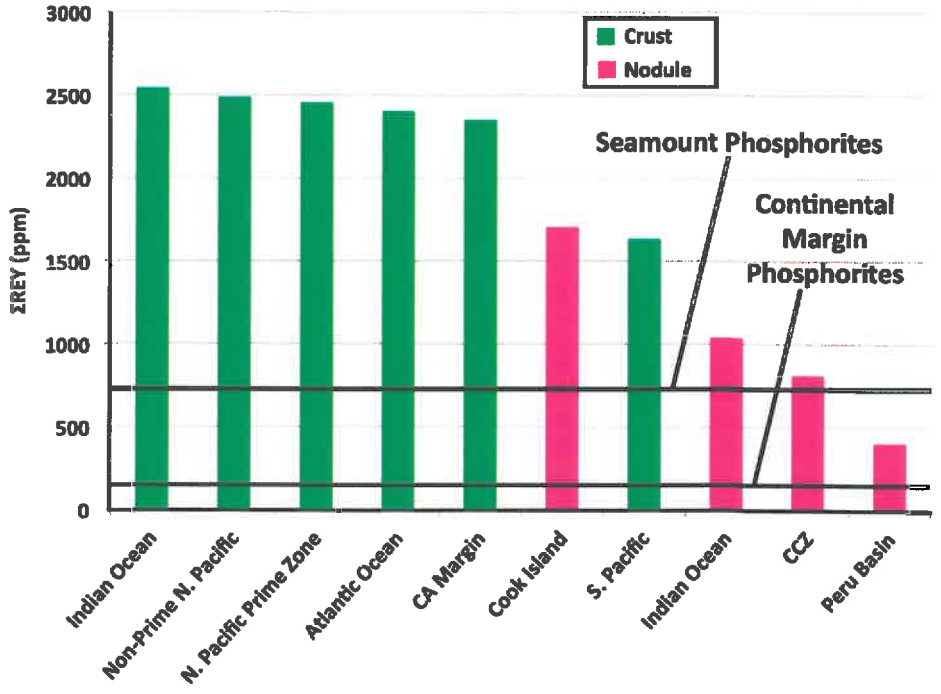

Figure 8. Bar diagram of mean total REY data for ferromanganese crusts and nodules compared to mean data for seamount and continental margin phosphorites.

An advantage to extracting REY from phosphorite deposits is that the REY are hosted by the CFA, which is easily dissolved with a mild acid leach [7]. This is not the case for land-based carbonatites, in which the REY are hosted in refractory minerals that are difficult to process. Given this processing advantage, and considering the relatively high grade and %HREY component, seamount phosphorite

deposits warrant further research as a potential future resource for REY. An exploration disadvantage for seamount phosphorites however is that they occur in the same places as Fe-Mn crusts on the seamounts and are typically covered by the Fe-Mn crusts. Consequently, it would require the development of new technology to identify phosphorite substrate rock beneath the Fe-Mn crusts, or detailed sampling.

In addition, it is because of this aspect of seamount phosphorites that reliable estimates of tonnages have not been possible to determine whereas tonnages are quite well known for some CM phosphorite deposits. An advantage of Fe-Mn crusts as a source for REY, like phosphorites, is that they also dissolve easily using a weak acid leach, and they are relatively accessible to exploration, although mining technology has yet to be fully developed. For crusts, the REY would be a byproduct of the mining of focus metals, such as Co, Ni, Mo, Mn, and others. The difficult aspect in development of a useful mining technology for crusts is the recovery of the Fe-Mn crust without also collecting substrate rock, which would dilute the grade of the ore. An ideal mine site might be one where the substrate rock is phosphorite. Then it would be desirable to collect both phosphorite and Fe-Mn crusts at the same time, which would provide two potential multi-component ore deposits in one mining operation, one with P and REY co-products and one with focus metals (Co, Ni, Mn) and byproducts (Mo, REY, Te, and others). Byproducts associated with phosphorite recovery are also possible, for example F, especially in seamount phosphorites, and U, V, and others in some CM deposits (Table S1). This would, however, complicate the processing and beneficiation, but is an option to consider during operational planning and exploration.

5. Conclusions

(1) Continental margin (CM) marine phosphorites have low total REY contents (mean 161 ppm) and high HREY complements (mean 49%), while seamount phosphorites have 4–6-times higher individual REY contents (except for Ce, which is comparable; mean ΣREY 727 ppm), and very high HREY complement (mean 60%).

(2) The predominant causes of higher concentrations and larger HREY complements in seamount phosphorites compared to CM phosphorites is the geological time of formation, changes in seawater REY concentrations over time, water depth of formation, differences in organic carbon content in the depositional environments and its role in the development of diagenetic zones in the sediment, and possibly the concurrent precipitation of Fe-Mn oxides with the seamount phosphorites.

(3) Fe-Mn crusts and nodules are another potential resource for REY. Both Fe-Mn deposit types have significantly lower HREY complements than the phosphorites and crusts have three to ten times higher REY concentrations. These differences can be explained by the mechanisms of incorporation of the REY into the mineral deposits: Predominantly sorption by the Fe-Mn oxides with surface oxidation of the Ce, and predominantly by substitution for Ca in the CFA structure, and to lesser extents by inheritance from the host rock and by sorption.

(4) Seamount phosphorites occur in the same places as Fe-Mn crusts on seamounts and the phosphorites are typically covered with Fe-Mn crusts, making exploration for phosphorites challenging. Consequently, it would require the development of new technology or detailed sampling to identify phosphorite substrate rock beneath the Fe-Mn crusts. Detailed sampling and geophysical measurements of a single guyot might provide geological or morphological criteria that would be useful for future exploration.

(5) An ideal mine site might be one where the substrate rock is phosphorite, in which case it would be desirable to collect both phosphorite and Fe-Mn crusts at the same time. This approach would provide two potential multi-component ore deposits in one mining operation, one with P and REY co-products and one with focus metals (Co, Ni, and Mn) and byproducts (e.g., Mo, REY, and Te).

(6) Potential ore deposits with high HREY complements, like the marine phosphorites analyzed in this paper, could help supply the HREY needed for high-tech and green-tech applications without creating an oversupply of the LREY. Consequently, a search for such deposits with the largest HREY/LREY ratios would help alleviate the supply/oversupply problem.

(7) Land-based phosphorite deposits offer a similar potential REY resource as a byproduct or co-product of the focus phosphate mining (e.g., [6,7]). Recovery of these land-based REY would require the addition of costly infrastructure and changes in extractive processing to the existing mining operations. Production of REY as a co-product of phosphorite mining would be advantageous if considered in the early stages of planning a new mining operation, such as those currently proposed for CM offshore sites.

Supplementary Materials: The following are available online at www.mdpi.com/2075-163X/6/3/88/s1, Table S1: Chemical composition of marine phosphorites, Figure S1: Photographs of continental margin phosphorites: (A) A pervasively Carbonate Fluorapatite (CFA)-replaced breccia, California margin; field of view represents 14 cm; (B) Phosphorite gravel with shell fragments from Chatham Rise, Table S2: Statistics of phosphorite deposits from continental margins, Table S3: Statistics of all phosphorite deposits from seamounts.

Acknowledgments: We thank the captain, ship's crew, and the scientific crew of the R.V. SP Lee Southern California Borderland cruises, 1974 and 1976, R.V. Gosnold Blake Plateau cruises, 1964 and 1965, Chain 46 Blake Plateau cruise, 1966, R.V. Atlantis II 266 Blake Plateau cruise, 1961, R.V. Seward Johnson and submersible Johnson Sea-Link Peru Margin expedition (SJ 1092), 1992, R.V. Robert D. Conrad Peru Margin cruise (23-06), 1982, R.V. Melville Majuro, Gilbert Islands, and Samoa cruise, 1999, R.V. Farnella Marshall Islands cruise, 1989, R.V. Farnella Hawaii cruise, 1989, R.V. Thomas G. Thompson Shatsky Rise cruise, 1994, R.V. Thomas Washington Northwest Pacific cruise, 1991, the R.V. Vinogradov Hawaii and Johnston Island cruise, 1991, R.V. Sonne 1 Southeast Pacific cruise, 1989/1990, R.V. Sonne 1 North Atlantic cruise, 1992, R.V. SP Lee Horizon Guyot, Necker Ridge, and Johnston Island cruise, 1983, R.V. Farnella Johnston Island and Karin Ridge cruise, 1986, and R.V. Farnella Hawaii cruise, 1988. We thank Ellen Roosen, WHOI and Brian Buczkowski, USGS for supplying Blake Plateau samples. We thank Lydia Somers for preparation and analysis of some of the seamount samples and Kira Arias La Rheir for preparation of samples. We thank the two anonymous reviewers and Amy Gartman, USGS, for useful comments that helped improve this paper.

Author Contributions: James R. Hein., Craig R. Glenn. and Ray Wood were responsible for collection of samples; James R. Hein, Andrea Koschinsky, Mariah Mikesell, and Kira Mizell for analyses of samples and data; and James R. Hein and Andrea Koschinsky for interpretation of data. All authors contributed to the final version of this manuscript.

Conflicts of Interest: The authors declare that the research was conducted in the absence of any commercial or financial relationships that could be construed as a potential conflict of interest. Any use of trade, product, or firm names is for descriptive purposes only and does not imply endorsement by the authors or their affiliated institutions.

References

1. Altschuler, Z.S. The geochemistry of trace elements in marine phosphorites Part I. Characteristic abundances and enrichment. In *Marine Phosphorites—Geochemistry, Occurrence, Genesis*; Bentor, Y.K., Ed.; Society of Economic Paleontologists and Mineralogists: Tulsa, OK, USA, 1980; pp. 19–30.
2. McArthur, J.M.; Walsh, J.N. Rare-earth geochemistry of phosphorites. *Chem. Geol.* **1984**, *47*, 191–220. [CrossRef]
3. Watkins, R.T.; Nathan, Y.; Bremner, J.M. Rare earth elements in phosphorite and associated sediment from the Namibian and South African continental shelves. *Mar. Geol.* **1995**, *129*, 111–128. [CrossRef]
4. Hein, J.R.; Yeh, H.-W.; Gunn, S.H.; Sliter, W.V.; Benninger, L.M.; Wang, C.-H. Two major Cenozoic episodes of phosphogenesis recorded in equatorial Pacific seamount deposits. *Paleoceanography* **1993**, *8*, 293–311. [CrossRef]
5. Glenn, C.R.; Föllmi, K.B.; Riggs, S.R.; Baturin, G.N.; Grimm, K.A.; Trappe, J.; Abed, A.M.; Galli-Olivier, C.; Garrison, R.E.; Ilyin, A.V.; et al. Phosphorus and phosphorites: Sedimentology and environments of formation. *Eclogae Geol. Helv.* **1994**, *87*, 747–788.
6. Christmann, P. A forward look into rare earth supply and demand: A role for sedimentary phosphate deposits? *Procedia Eng.* **2014**, *83*, 19–26. [CrossRef]
7. Emsbo, P.; McLaughlin, P.I.; Breit, G.N.; du Bray, E.A.; Koenig, A.E. Rare earth elements in sedimentary phosphate deposits: Solution to the global REE crisis? *Gondwana Res.* **2015**, *27*, 776–785. [CrossRef]

8. Santos, A.J.G.; Mazzilli, B.P.; Fávaro, D.I.T.; Silva, P.S.C. Partitioning of radionuclides and trace elements in phosphogypsum and its source material based on sequential extraction methods. *J. Environ. Radioact.* **2006**, *87*, 52–61. [CrossRef] [PubMed]
9. Weng, Z.; Jowitt, S.M.; Mudd, G.M.; Haque, N. A detailed assessment of global rare earth element resources: Opportunities and challenges. *Econ. Geol.* **2015**, *110*, 1925–1952. [CrossRef]
10. Koschinsky, A.; Stascheit, A.; Bau, M.; Halbach, P. Effects of phosphatization on the geochemical and mineralogical composition of marine ferromanganese crusts. *Geochim. Cosmochim. Acta* **1997**, *61*, 4079–4094. [CrossRef]
11. Glenn, C.R.; Arthur, M.A. Petrology and major element geochemistry of Peru margin phosphorites and associated diagenetic minerals: Authigenesis in modern organic-rich sediments. *Mar. Geol.* **1988**, *80*, 231–267. [CrossRef]
12. Glenn, C.R.; Arthur, M.A.; Resig, J.M.; Burnett, W.C.; Dean, W.E.; Jahnke, R.A. Are Modern and Ancient Phosphorites Really So Different? In *Siliceous, Phosphatic and Glauconitic Sediments of the Tertiary and Mesozoic*; Iijima, A., Abed, A.M., Garrison, R.E., Eds.; VSP International Science Publishers: Leiden, The Netherlands, 1994; pp. 159–188.
13. Kudrass, H.; Cullen, D. Submarine phosphorite nodules from the Central Chatham Rise off NZ-composition, distribution and reserves—(Valdivia Cruise 1978). *Geol. Jahrb.* **1982**, *D51*, 3–41.
14. Cook, H.E.; Johnson, P.D.; Matti, J.C.; Zemmels, I. Methods of sample preparation and X-ray diffraction data analysis (X-ray mineralogy laboratory, Deep Sea Drilling Project, University of California Riverside). In *Initial Reports of the Deep Sea Drilling Project*; U.S. Government Printing Office: Washington, DC, USA, 1975; Volume 28, pp. 999–1007.
15. Hein, J.R.; Schwab, W.C.; Davis, A.S. Cobalt and platinum-rich ferromanganese crusts and associated substrate rocks from the Marshall Islands. *Mar. Geol.* **1988**, *78*, 255–283. [CrossRef]
16. McLennan, S.M. Rare earth elements in sedimentary rocks: Influence of provenance and sedimentary processes. In *Geochemistry and Mineralogy of Rare Earth Elements*; Lipin, B.R., McKay, G.A., Eds.; Mineralogical Society of America's Reviews in Mineralogy: Washington, DC, USA, 1989; Volume 21, pp. 169–200.
17. Anders, E.; Grevesse, N. Abundances of the elements: Meteoritic and solar. *Geochim. Cosmochim. Acta* **1989**, *53*, 197–214. [CrossRef]
18. Bau, M.; Koschinsky, A.; Dulski, P.; Hein, J.R. Comparison of the partitioning behaviours of yttrium, rare earth elements, and titanium between hydrogenetic marine ferromanganese crusts and seawater. *Geochim. Cosmochim. Acta* **1996**, *60*, 1709–1725. [CrossRef]
19. Alibo, D.S.; Nozaki, Y. Rare earth elements in seawater: Particle association, shale-normalization, and Ce oxidation. *Geochim. Cosmochim. Acta* **1999**, *63*, 363–372. [CrossRef]
20. Hughes, J.M.; Cameron, M.; Mariano, A.N. Rare-earth-element ordering and structural variations in natural rare-earth-bearing apatites. *Am. Mineral.* **1991**, *76*, 1165–1173.
21. Hughes, J.M.; Rakovan, J.F. Structurally robust, chemically diverse: Apatite and apatite supergroup minerals. *Elements* **2015**, *11*, 165–170. [CrossRef]
22. Piper, D.Z.; Perkins, R.B.; Rowe, H.D. Rare-earth elements in the Permian Phosphoria Formation: Paleo proxies of ocean geochemistry. *Deep Sea Res. II* **2007**, *54*, 1396–1413. [CrossRef]
23. De Baar, H.J.W.; Bacon, M.P.; Brewer, P.G.; Bruland, K.W. Rare earth elements in the Pacific and Atlantic Oceans. *Geochim. Cosmochim. Acta* **1985**, *49*, 1943–1959. [CrossRef]
24. Zhang, J.; Nozaki, Y. Rare earth element and yttrium in seawater: ICP-MS determination in the East Caroline, Coral Sea, and South Fiji basins of the western South Pacific Ocean. *Geochim. Cosmochim. Acta* **1996**, *60*, 4631–4644. [CrossRef]
25. Lécuyer, C.; Reynard, B.; Grandjean, P. Rare earth element evolution of Phanerozoic seawater recorded in biogenic apatites. *Chem. Geol.* **2004**, *204*, 63–102. [CrossRef]
26. Hein, J.R.; Conrad, T.A.; Dunham, R.E. Seamount characteristics and mine-site model applied to exploration- and mining-lease-block selection for cobalt-rich ferromanganese crusts. *Mar. Georesour. Geotechnol.* **2009**, *27*, 160–176. [CrossRef]
27. Hein, J.R.; Mizell, K.; Koschinsky, A.; Conrad, T.A. Deep-ocean mineral deposits as a source of critical metals for high- and green-technology applications: Comparison with land-based deposits. *Ore Geol. Rev.* **2013**, *51*, 1–14. [CrossRef]
28. Baturin, G.N. Thallium in oceanic phosphorites. *Dokl. Earth Sci.* **2004**, *394*, 68–72.

29. Benninger, L.M.; Hein, J.R. Diagenetic evolution of seamount phosphorite. In *Marine Authigenesis: From Global to Microbial*; Glenn, C.R., Prévôt-Lucas, L., Lucas, J., Eds.; SEPM Special Publication: Tulsa, OK, USA, 2000; pp. 245–256.
30. Jarvis, I.; Burnett, W.C.; Nathan, Y.; Almbaydin, F.S.M.; Attia, A.K.M.; Castro, L.N.; Flicoteaux, R.; Hilmy, M.E.; Husain, V.; Quatawnah, A.A.; et al. Phosphorite geochemistry: State-of-the-art and environmental concerns. *Eclogae Geol. Helv.* **1994**, *87*, 643–700.
31. Long, K.R.; van Gosen, B.S.; Foley, N.K.; Cordier, D. *The Principal Rare Earth Elements Deposits of the United States—A Summary of Domestic Deposits and a Global Perspective*; U.S. Geological Survey Scientific Investigations Report 2010-5220; U.S. Geological Survey: Reston, VA, USA, 2010; p. 96.
32. Hein, J.R. *Prospects for Rare Earth Elements from Marine Minerals*; International Seabed Authority Briefing Paper 02/12; International Seabed Authority: Kingston, Jamaica, 2012; pp. 1–4.
33. Hein, J.R.; Koschinsky, A. Deep-ocean ferromanganese crusts and nodules. In *Treatise on Geochemistry*, 2nd ed.; Holland, H.D., Turekian, K.K., Eds.; Elsevier: Oxford, UK, 2014; Volume 13, Chapter 11; pp. 273–291.
34. Hein, J.R.; Spinardi, F.; Okamoto, N.; Mizell, K.; Thorburn, D.; Tawake, A. Critical metals in manganese nodules from the Cook Islands EEZ, abundances and distributions. *Ore Geol. Rev.* **2015**, *68*, 97–116. [CrossRef]
35. Stegen, K.S. Heavy rare earths, permanent magnets, and renewable energies: An imminent crisis. *Energy Policy* **2015**, *79*, 1–8. [CrossRef]